BROADBAND DYNAMIC SOURCE MODEL FOR THE 2011 TOHOKU EARTHQUAKE USING SLIP REACTIVATION AND EGF SIMULATION

P. GALVEZ[1,4], A. PETUKHIN[2], K. IRIKURA[3], P. SOMERVILLE[4]

[1] King Abdullah University of Science and Technology (KAUST), Thuwal, Saudi Arabia

[2] Geo-Research Institute, Osaka, Japan

[3] Aichi Institute of Technology, Toyota, Japan

[4] AECOM, Los Angeles, USA

E-mail contact of main author: percy.galvez.barron@gmail.com

Abstract. This paper describes a validated dynamic rupture model of the 2011 Tohoku earthquake that reproduces both long-period (20-100sec) and short period (3-20sec) ground motions. The purpose of the study is to gain insight into parameters, such as slip time functions, that are poorly resolved by source inversions. In order to reproduce the observed large slip area (slip asperity) we assign a large Dc area following kinematic source inversion results. Sufficiently large slip was achieved through rupture reactivation by the double-slip-weakening friction model. In order to reproduce strong-motion generation areas (SMGAs), we assign short *Dc* and large stress-drop areas following EGF simulation results, which indicate that although more distant from the hypocenter, SMGA1 ruptured earlier than SMGA2 or SMGA3, which are closer to the hypocenter. This observation is confirmed by the back-projection method (Meng et al, 2011[9]). In order to reproduce this important feature in dynamic simulation results, we introduced a chain of small high stress-drop patches between the hypocenter and SMGA1, leading to rupture from the hypocenter to SMGA1. By the systematic adjustment of stress drops and slip critical distance (*Dc*) values, the rupture reproduces the observed sequence and timing of SMGA ruptures and the final slip derived by kinematic models.

This model also reproduces the multi-seismic wave front observed from strong ground motion data recorded along the Pacific coast of the Tohoku region. We compare the velocity waveforms recorded at rock sites along the coastline with 1D synthetic seismograms for periods of 20-100s. The fit is very good at stations in the northern and central areas of Tohoku. We also perform 3DFDM simulations for periods of 5-20s, and confirm that our dynamic model also reproduces wave envelopes in northern and central Tohoku. Overall, we are able to validate the rupture process of the Tohoku earthquake.

Key Words: 2011 Tohoku earthquake, dynamic simulation, rupture propagation, slip reactivation

1. Introduction

The March 11th, 2011, Mw 9 Tohoku earthquake occurred in the subduction zone, between the Pacific and North American plates in northeastern Honshu, Japan. This giant event was recorded by a vast GPS and seismic network. The Tohoku earthquake featured complex rupture patterns involving multiple rupture fronts. Numerous source models have been generated using extensive teleseismic, GPS, strong ground motion, and tsunami data (see review Tajima et al. 2013[1], and Lay, 2017[2], for the most recent results).

Visual inspection of the short-period strong ground motion recorded by the K-NET and KiK-net networks and the high-rate 1 Hz GPS long-period displacements recorded by the

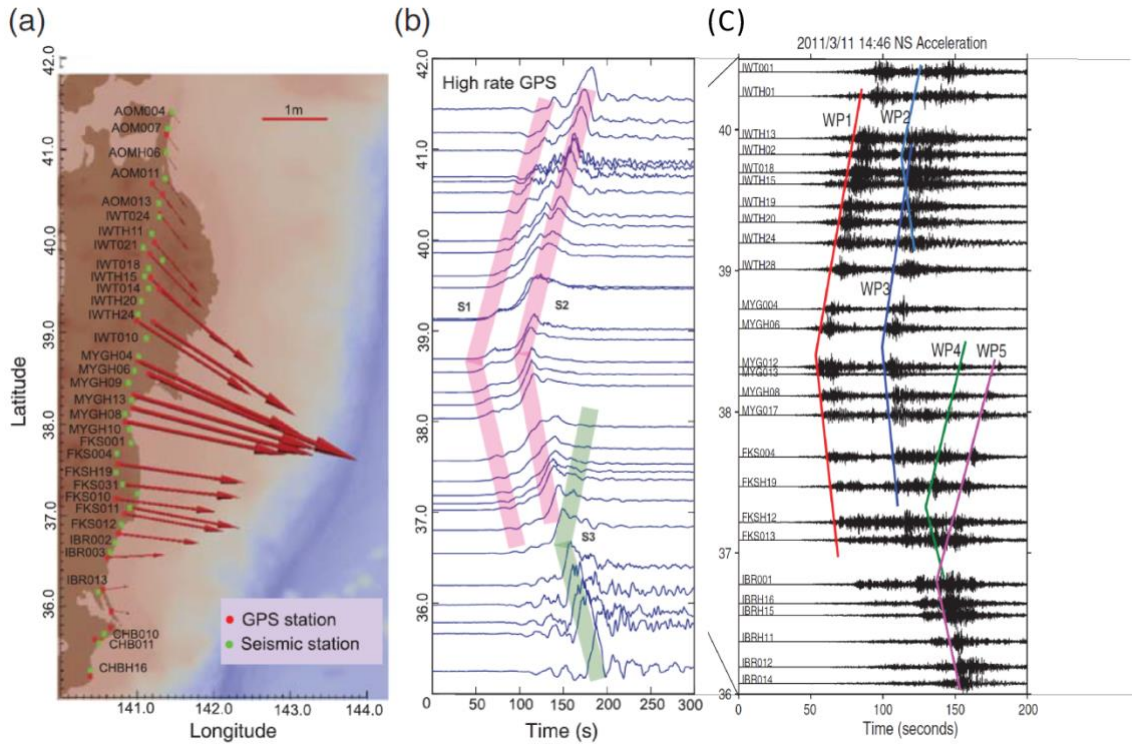

FIG. 1. The green and read squares are the seismic and GPS stations respectively. The red arrow are the coseismic displacements generated during Tohoku earthquake. (b) High-rate continuous GPS records sampled at 1 Hz from the GEONET network. The transparent red lines delineates the first (S1) and second seismic wave fronts (S2) observed in the records. The green line (S3) highlights the third pulse observed in the southern part. (c) The strong ground motion recorded from (Kik-net and K-NET) networks between 0 and 3 Hz. Colored lines denotes wave packets WP1-WP5 identified by Kurahashi and Irikura, 2013[3]..

GEONET network along the Japanese coast clearly show several groups of waves. Two long-period groups of waves (S1 and S2 in FIG. 1) arrive about 40-50 seconds apart in both the Miyagi and Iwate regions. A third group of waves (S3 in FIG. 1) is observed further south in the Ibaraki and Chiba regions. Short-period ground motions have a more complicated pattern: five wave packets (WP1-WP5 in FIG. 1) were identified by Kurahashi and Irikura, 2013[3]. These observations indicate that the Tohoku earthquake featured complex rupture patterns involving multiple rupture fronts. Kurahashi and Irikura (2011, 2013)[4,3] found that these multiple wave fronts were generated by strong ground motion areas (SMGAs) located in the deep region of the plate interface.

There is strong evidence that the fault regions that generate short-period and long-period wave radiation during a given earthquake are spatially distinct. The most direct observations of this phenomenon have been obtained for large subduction earthquakes, for which the combination of geodetic, tsunami, strong motion and teleseismic data (including back-projection of high-frequency teleseismic data from large arrays) provides adequate spatial resolution on the location of slip at different frequencies (e.g. Tohoku 2011: Kubo et al., 2013, Yoshida et al., 2011, Kurahashi and Irikura, 2013[5, 6, 3]). Other related observations include a lack of coincidence between the timing of low and high frequency wave amplitudes in teleseismic data (e.g. Gusev et al., 2006[7]). A statistical analysis of kinematic finite source models inferred from geophysical data reveals that areas of large final slip (long-period generation areas) and areas of large peak slip rate (short-period generation areas) are spatially distinct (Simons et al., 2011; Meng et al., 2011; Huang et al., 2013, 2014; Galvez et al., 2014,

2016; Avouac et al., 2015[8, 9, 10, 11, 12, 13, 14]). This feature has important implications for procedures adopted for the prediction of strong ground motion. In particular, it is not incorporated in many kinematic/stochastic source models developed for engineering applications that assume that high-frequency radiation is uniformly distributed over the rupture area or correlated with the spatial distribution of final slip (e.g. Somerville et al., 1999, Irikura and Miyake, 2001[15, 16]).

One plausible explanation for the discrepancy between short-period and long-period generation areas is based on the spatial heterogeneity of stress and strength (frictional parameters) along the fault. In fundamental models of earthquake dynamics based on classical fracture mechanics, high-frequency radiation is most efficiently generated by abrupt changes of rupture speed (e.g. Madariaga, 1977, Pulido and Dalguer, 2009[17, 18]) induced by the residual stress concentrations left by previous slip events, or by sharp spatial contrasts of fracture energy due to heterogeneities of friction properties or effective normal stress (Huang et al., 2013, 2014; Galvez et al., 2014, 2016[10, 11, 12, 13]). High frequency radiation is also enhanced by short rise time (the duration of slip at a given point on the fault, e.g. Nakamura and Miyatake, 2000, Hisada 2000, 2001, Guatteri et al., 2003[19, 20, 21, 22]) which can be controlled by a number of processes, such as frictional velocity-weakening parameters, characteristic width of asperities, and thickness of a damaged fault zone (Heaton., 1990, Perrin, 1995, Beroza and Mikumo, 1996, Huang and Ampuero, 2011[23, 24, 25, 26]).

In order to simulate dynamic earthquake rupture and strong ground motion in realistic models that include crustal heterogeneities and complex fault geometries, which is an important goal of computational seismology, Galvez et al., 2014[12], incorporate dynamic rupture modelling capabilities in a spectral element solver on unstructured meshes, the 3-D code SPECFEM3D. This tool provides high flexibility in representing fault systems with complex geometries, including non-planar faults and sharp wedges. The domain size is extended with progressive mesh coarsening to maintain an accurate resolution of the static field. They present a conceptual minimalistic dynamic rupture model of the 2011 Mw 9.0 Tohoku earthquake including a non-planar plate interface with heterogeneous frictional properties and initial stresses. The model is consistent with depth-dependent frequency content of slip, where the shallow part radiates coherent energy at low frequency (kinematic source inversions, tsunami models) and the deep part radiates at high frequency (back projection of HF radiation). The deep HF radiation is interpreted as the rupture of high stress drop patches in the bottom part of the seismogenic zone of the megathrust (e.g. Huang et al. 2012; Lay et al. 2012[27, 28]). The model parameters are assigned by systematic trials, taking as a starting point the 2-D dynamic rupture models developed by Huang et al., 2012[27]. The simulation results of Galvez et al., 2014[12] qualitatively reproduce the depth-dependent frequency content of the source and the large slip close to the trench observed in the Tohoku earthquake.

Galvez et al., 2016[13], developed a new rupture reactivation model based on a double-slip-weakening friction law similar to that introduced by Kanamori and Heaton, 2000[29]. These authors proposed that melting or fluid pressurization induced by frictional heating can reduce fault strength when slip exceeds a certain critical slip distance (Dr). They argued that, when superimposed to the conventional (isothermal) slip-weakening process with shorter critical slip distance (Dc), these thermally activated weakening mechanisms lead to a slip-dependent friction model with two sequential strength drops.

The main goal of Galvez et al., 2016[13] was to show that the double slip-weakening friction in the form proposed by Kanamori and Heaton, 2000[29] offers a plausible model for the rupture process of the 2011 Tohoku earthquake, including large shallow slip, rupture reactivation, and

large rupture extent. They present evidence supporting this friction model, obtained from seismological observations, laboratory experiments, and theoretical considerations. Then, they extend the dynamic rupture model developed by Galvez et al., 2014[12] by modifying the slip-weakening friction model to account for rupture reactivation. Finally, they show that this model produces (1) a rupture pattern consistent with a kinematic source inversion model that features rupture reactivation and (2) ground-motion patterns along the Japanese coast consistent with the observations, namely, two groups of long-period seismic waves.

In order to reproduce the large rupture extent and the depth-dependent frequency content qualitatively, Galvez et al., 2014; 2016[12, 13], used cloudy distributions of high stress drop patches in the deep part of the megathrust, following the back projection results of Meng et al., 2011[9]. In contrast, Kurahashi and Irikura, 2011, 2013[4,3] (as well as Asano and Iwata, 2012, Satoh, 2012, and Kawabe and Kamae, 2013[30, 31, 32]), used empirical Green's function (EGF) simulations and demonstrated that strong ground motions can be reproduced by a model having only five compact SMGAs, numbered SMGA1-SMGA5 in accordance with their rupture time. From the rupture dynamics point of view, a problem of the EGF results is that hypocenter, SMGA1 and SMGA3 are located approximately on the same east-west line but in a reverse order of timing: SMGA1, which ruptured first, is far from the hypocenter, while SMGA3, which is between the hypocenter and SMGA1, ruptured after SMGA1, as shown in FIG. 2.

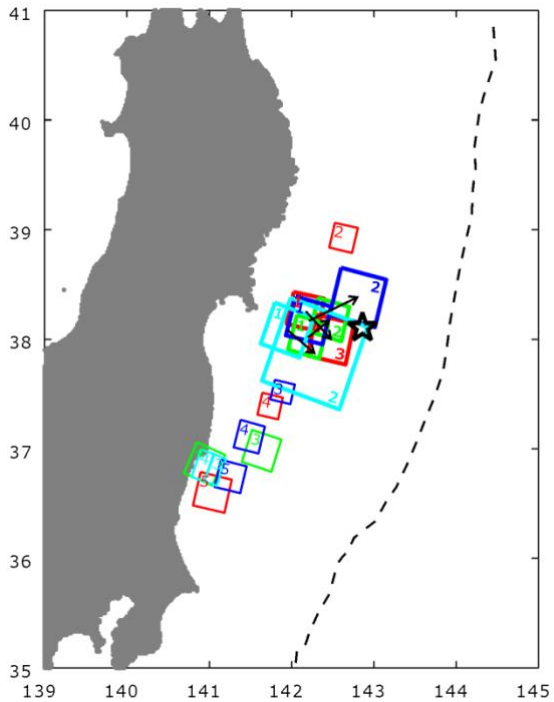

FIG. 2. Distribution of SMGA areas of the 2011 Tohoku earthquake. Rectangular areas are SMGAs according to the EGF analysis of Kurahashi and Irikura, 2013[3] (red), Asano and Iwata, 2012[30], (green) Kawabe and Kamae, 2013[32] (blue), and Satoh 2012[31] (light blue). The numbers assigned to the SMGA's correspond to their rupture sequence. Arrows indicate reverse sequence from SMGA1 to subsequent SMGA2 or SMGA3. The star marks the earthquake epicenter.

In this study we modify the dynamic model of the 2011 Tohoku earthquake developed earlier in by Galvez et al., 2014; 2016[12, 13], in order to obtain good agreement between simulated and recorded strong motion waveforms, between dynamically modelled slip and slip distribution estimated by kinematic source inversion, and finally between dynamically modelled and EGF modelled SMGA rupture time. The improved dynamic model of the 2011 Tohoku earthquake has five SMGAs in the deeper part (consistent with Kurahashi and Irikura, 2013[3]) and one large slip area in the shallower part of the fault.

We extract the dynamic source parameters, slip velocity or moment rate function, at each grid point on the fault and use them in calculating the strong ground motions of the Tohoku earthquake using 3D-FDM. The results are compared with the observed waveforms.

Our goal is to understand the mechanical origin of the phenomenon at a sufficient level to provide a physical basis for the formulation of simplified methods to account for distinct short- and long-period slip in kinematic or pseudo-dynamic earthquake source generation algorithms for engineering ground motion prediction.

2. Dynamic model settings

Following the asperity model presented by Galvez et al., 2016[13], we present a minimalistic dynamic rupture model with slip reactivation. The tool used to simulate rupture process for the 2011 Tohoku earthquake is SPECFEM3D with the recent dynamic rupture module implemented by Galvez et al., 2014[12]. The intra-slab fault geometry has been adapted from Simons et al., 2011[8], taking into account the folded slab interface including the small angles in the wedge close to the trench. The state-of-the-art unstructured mesh software CUBIT provides a powerful tool to deal with geometrical complexities. We use these capabilities to perform dynamic rupture simulation for the Tohoku earthquake including the non-planar slab interface and small angles (<5 degrees) found in the trench wedge, see FIG. 3. The velocity structure is a 1D layered medium taken from Fukuyama et al., 1998[33], see TABLE 1. Based on this non-planar fault geometry, we assign asperities and SMGAs following the source inversion results and gradually modify the asperity distribution.

To create more slip in the shallow regions, the main asperity was moved closer to the trench in comparison with Galvez et al., 2016[13]. Many kinematic models has been generated by seismic inversion for the 2011 Tohoku earthquake and most of them unequivocally reveal a shallow region (< 20 km) of large slip (> 40 m) close to the trench (e.g. Lee et al. 2011; Yue and Lay 2011; Suzuki et al. 2011; Yagi and Fukahata 2011; Yoshida et al., 2011; Wei et al. 2012[34, 35, 36, 37, 6, 38]). Models of this type are supported by tsunami inversion (e.g. Satake et al., 2013, Gusman et al., 2012[39, 40]) or are able to reproduce tsunami by themselves (e.g. Yamazaki, 2013, Petukhin et al., 2017[41, 42]). Here we follow the final slip model of Lee et al., 2011[33] (see FIG. 7 below) and place a semi-elliptical asperity closer to the trench, delimitating the region of large slip (FIG. 4).

In deeper regions between 30 to 50 km depth, high frequency radiation has been detected by empirical Green's function techniques (EGF, e.g. Kurahashi and Irikura, 2011; 2013, Asano and Iwata, 2012[4, 3, 30]), and also back projection techniques (e.g. Meng et al. 2011; Ishii, 2011; Yagi et al. 2012[9, 43, 44]) possibly explained by the presence of prior small asperities from historical earthquakes (Ide and Aochi 2013[45]) that broke again during the Tohoku earthquake. We place deep asperities on the detected SMGAs, close to the positions identified by Kurahashi and Irikura, 2013[3] and other researchers; see FIG. 4.

The slip weakening friction law is assumed. By the systematic adjustment of stress drops and slip critical distance (Dc) values, the rupture reproduces the final slip derived by kinematic models (e.g. Suzuki et al., 2011; Lee et al., 2011[36, 34]). Around 20 models were investigated in total. In FIG. 5 the frictional parameter settings, and in FIG. 4 the stress drop (To-Td) are shown.

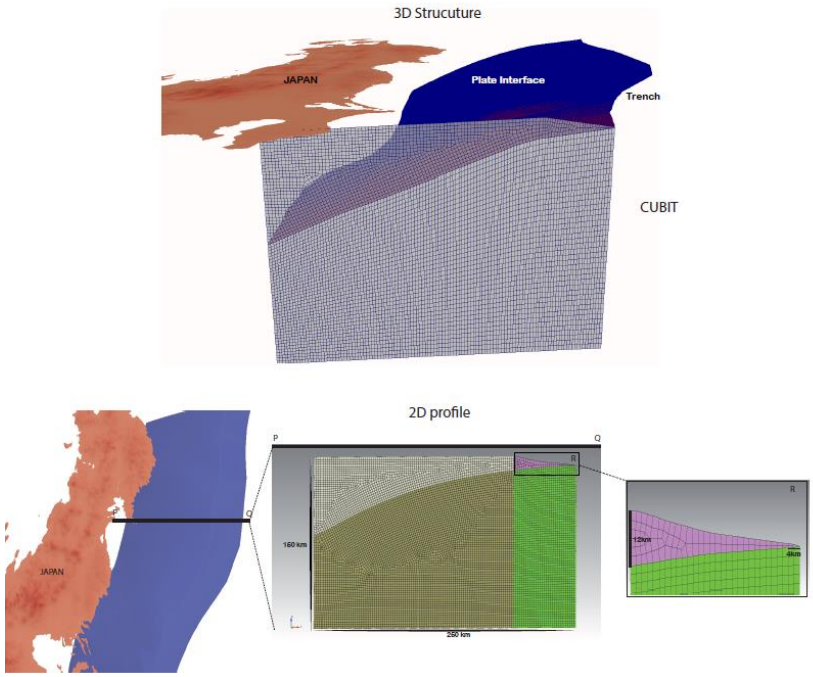

FIG. 3. The blue non-planar interface adapted from Simons et al., 2011[8] is the fault geometry used in our model. The vertical brown plane is the vertical section of the volume meshed by CUBIT. (b) 'PQ' is a profile cutting the mesh. The rectangle 'R' is the zoom in region close to the trench. Tiny angles (< 5 degrees) could be meshed.

TABLE 1**:** ONE DIMENSIONAL VELOCITY STRUCTURE USED IN DYNAMIC SIMULATION.

Thickness (m)	**P-velocity (m/s)**	**S-velocity (m/s)**	**Density (kg/m^3)**
3000	5500	3140	2300
15000	6000	3550	2400
15000	6700	3830	2800
67000	7800	4460	3200
inf	8000	4570	3300

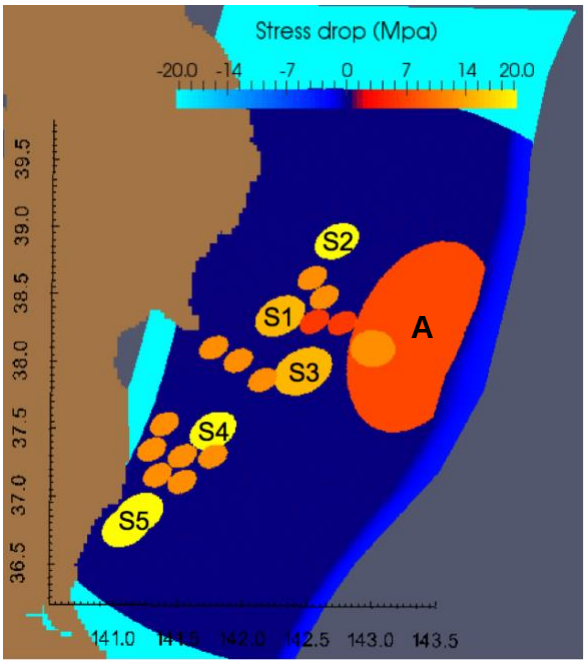

FIG. 4. Asperity and stress drop distribution. The circles labeled "S1-S5" are located on the SMGA regions found by Kurahashi and Irikura, 2013[3]. Asperity A has been placed on a region of large slip revealed by the kinematic models. The chain of two high stress drop spots (bridge) between the rupture initiation area (orange colored spot inside asperity A) and S1 on this and previous figures was introduced in order to drive rupture to S1 first in accordance with the rupture sequence in Figures 1 and 2.

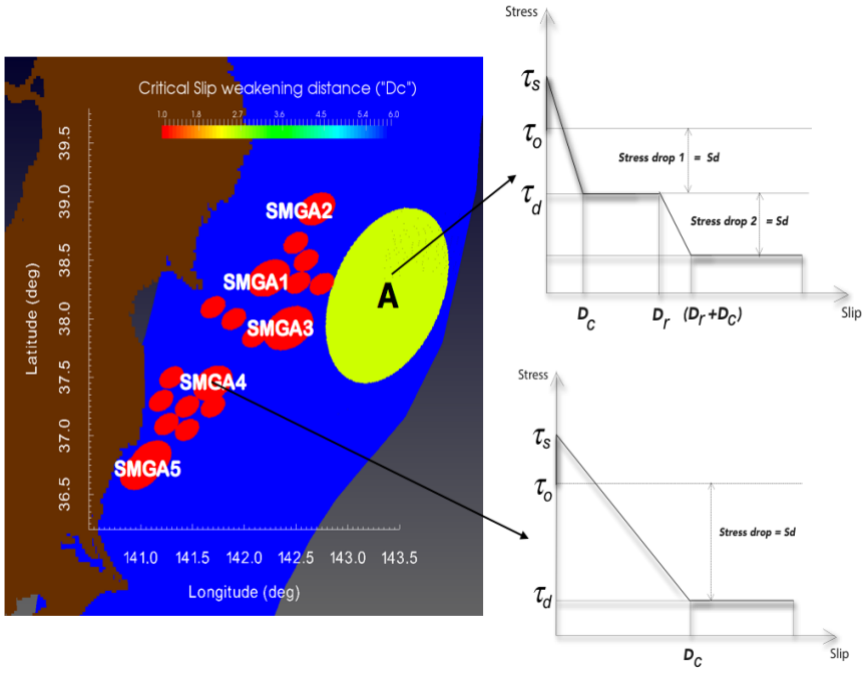

FIG. 5. Slip critical distance and friction law used by this model. The asperity (A) follows a slip weakening distance friction with two stress drop steps. In this constitutive friction law, the stress drops a second time once the slip reaches a critical distance (Dr). In the deeper asperities, a slip weakening friction law has been prescribed with only one stress drop step.

2.1.Friction model settings for asperity A: slip reactivation

Following Galvez et al., 2016[13], reactivation by the double-slip-weakening friction model was considered in this study. Evidence of a slip reactivation process, first proposed by Kanamori and Heaton, 2000[29], has been reported by Lee et al., 2011[34] for the Tohoku earthquake, and by laboratory rock experiments (O'Hara et al., 2006[46]), although the relevance of experimental material to the fault material is unclear. According to this experiment, during faulting the fault surfaces reach high temperature and decay emanating CO2 (thermal decomposition). This thermal decomposition process generates nano-layers of soft material weakening the fault once again. The experiment recorded 4 stages of friction. In stage I and II, the friction coefficient decreases (first weakening) during the first 2-5 meters of slip. In stage III, the friction initially remains constant but after 20-25 meters of slip a second reduction in friction occurs. This second drop of friction may have produced the slip reactivation process that evidently occurred during Tohoku earthquake. Experiments on a more relevant granitic rock were made recently by Chen et al., 2017[47]. These experiments also reveal a second friction drop due to melting at large slip.

The kinematic model of Lee et al., 2011[34] shows a predominant repeating slip patch close to the hypocenter. This model inverted teleseismic, local dense strong ground motion and near-field coseismic geodetic data covering a broad frequency range that allowed the details of the megathrust earthquake rupture to be resolved. The inversion method made use of multiple time windows and took advantage of robust data and powerful parallel computing techniques to achieve a high resolution source inversion. Lee's model shows a slip reactivation on the largest asperity close to the trench. To illustrate the rupture reactivation, Galvez et al., 2016[13], took a sequence of slip-velocity snapshots and stacked the slip velocity on the fault at locations crossing the hypocenter. The stacking of slip velocities along these locations reveals two ruptures, both initiating close to the hypocentre, separated by about 40-50 seconds. The first rupture propagates mainly towards the trench and the second rupture propagates bilaterally with one front moving towards the trench and the other front moving down-dip.

Galvez et al., 2016[13] also computed the dynamic fault stress changes implied by the Lee et al., 2011[34] kinematic source model by applying its spatiotemporal distribution of slip velocity as a boundary condition along the fault in a spectral element seismic-wave propagation simulation done with the SPECFEM3D code. The stress change features two sequential drops, correlated in time with two peaks of slip velocity. In particular, it shows that the critical slip for the onset of the second weakening is Dr ≈ 20 m in the hypocentral region (FIG. 6a). The second stress drop starts at 40 seconds when the slip reaches 20 m and the slip rates increases again. This second stress drop causes the slip rupture reactivation. There is a step in the stress versus slip function. This stress-slip step function has been adapted to a simple linear slip-weakening friction law where the friction decays linearly to a critical slip weakening distance (Dc) and after reaching a threshold slip (Dr), the friction decreases again (FIG. 6b).

This model qualitatively reproduces the multi-seismic wave front observed in the strong ground motion and GPS data along the Japanese coast (FIG. 1). The fitting of the recorded velocity waveform with our 1D synthetic between 20 to 100 seconds period is very good at this station but not this good at other stations.

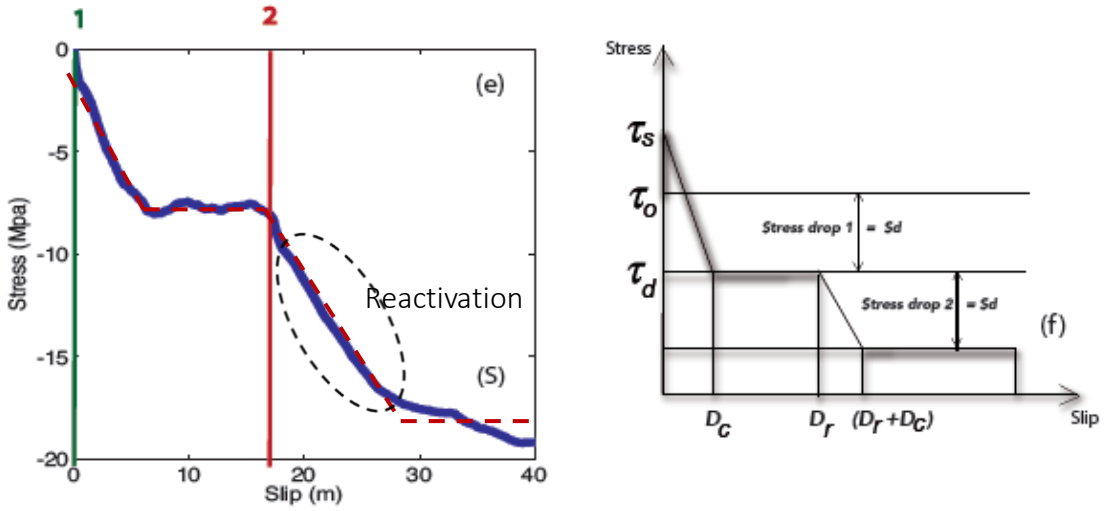

FIG. 6. (a) Step-stress-slip distribution at a point close to the hypocenter computed from the slip-rate snapshots of Lee et al., 2011[34]; dashed ellipse indicates stress drop related to the rupture reactivation. (b) Sketch of the stress-slip relation used in the dynamic model.

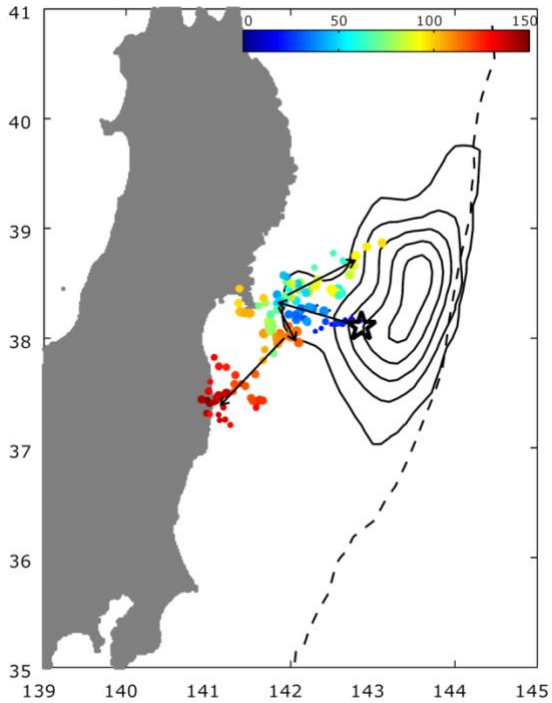

FIG. 7. Source area of the 2011 Tohoku earthquake. Contours represent the slip distribution according to a kinematic source inversion (Lee et al., 2011[34]). Dots are high-frequency radiators according to the back-projection analysis of Meng et al, 2011[9] reduced from USGS to the JMA epicenter location. Color of dots denotes timing with respect to the source time; size of dots denotes radiation amplitudes. Arrows indicate propagation of high-frequency radiator. The reverse character of the propagation is similar to the rupture sequence of SMGAs in FIG. 1.

2.2.Distribution of SMGAs and smaller asperities: bridge of small asperities

Based on the observations of Kurahashi and Irikura, 2013[3], we placed small SMGAs at a depth of around 30 km along the intra-slab interface, denoted by SMGA1~SMGA5 according to their rupture sequence, as shown in FIG. 5.

Using EGF simulations, Kurahashi and Irikura, 2013[3] (see also Kawabe et al., 2011, Asano and Iwata, 2012[32, 30]) observed a reverse rupture sequence of SMGAs: Hypocenter-SMGA1-SMGA2-SMGA3, see FIG. 2. In order to reproduce this anomalous SMGA strong motion radiation sequence, we need to try specific SMGA settings, like the example in FIG. 4, where small patches having high stress-drop drive rupture to SMGA1 first, and then let rupture propagate to SMGA2 and SMGA3 in the order found by Kurahashi and Irikura, 2013[3].

FIG. 7 demonstrates observational evidence for the bridge in the back projection result of Meng et al., 2011[9], which indicates a chain of bursts of high-frequency radiation from the hypocenter to the west (chain of blue dots marked by the first arrow).

2.3.Dynamic simulation results (periods 20-100 sec)

For efficiency, SPEC3FDM requires large meshes for regions outside the rupture zones. As a result, waveforms produced by dynamic simulation are valid in the long-period range: 20 - 100 sec. The dynamic model including the SMGA regions radiates a complex seismic wave field. FIG. 8 shows snapshots of rupture propagation. In the first 20 seconds, the rupture initially propagates up-dip towards the trench, and between 30 to 40 seconds a down-dip rupture front breaks the SMGA1 asperity.

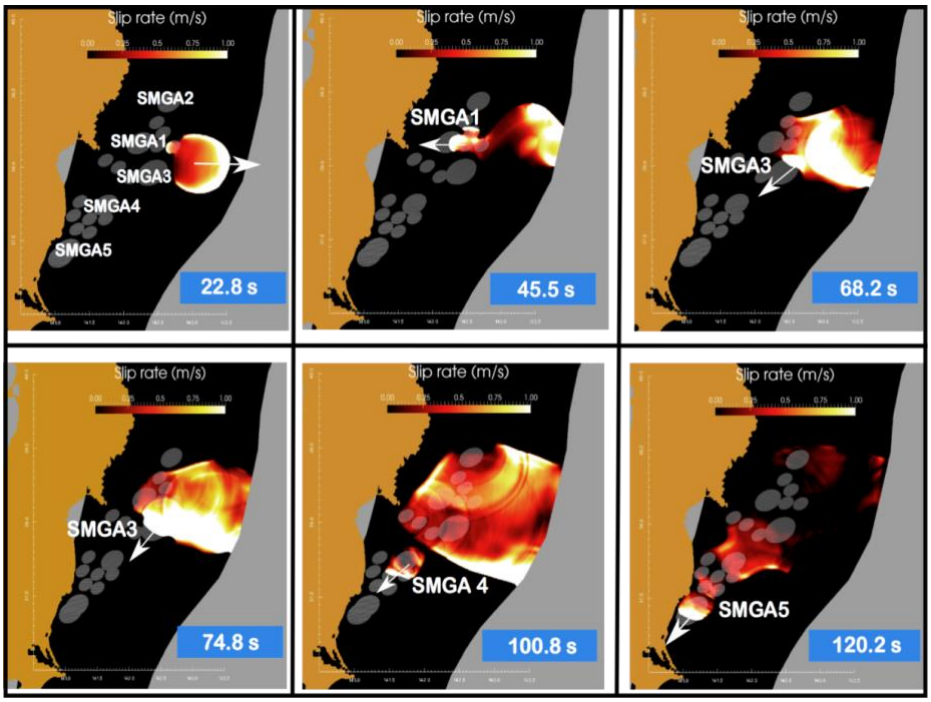

FIG. 8. Slip-rate snapshots showing the rupture sequence. Initially the rupture propagates to the trench and a down-dip rupture front appears at 22.8 seconds and starts to break the SMGA1 asperity at between 40 to 45.5 seconds. During this time the up-dip rupture reactivates close to the trench and generates a second rupture front strong enough to break SMGA3 at 68.2 seconds. At 100.8 seconds the southward rupture propagation breaks SMGA4 and finally activates SMGA5 at 120.2 seconds.

During up-dip propagation, the rupture reactivates, strongly breaking the trench and generating a second rupture front with enough energy to rupture SMGA3 at 68.2 seconds. Subsequently the rupture propagates northwest activating SMGA2 between 75 to 80 seconds. In the southward propagation, the rupture breaks SMGA4 at 100 seconds and travels further to finally activate SMGA5 at 120 seconds. The rupture time is shown in FIG. 9.

Supplementary animation of seismic wave propagation shows the multi-seismic wave fronts that arrive at the seismic stations along the Japanese coast. In the first 30 seconds the up-dip rupture radiates an energetic seismic wave field towards the trench but radiates weak seismic waves toward the land. In fact the waves die out before arriving at the Japanese coast. The first strong seismic waves onshore appear once the down-dip rupture starts breaking the SMGAs. These SMGA asperities have enough stress drop to radiate seismic waves that are detected by the seismic stations along the Japanese coast. In FIG. 10 recorded and synthetic waveforms at the Japanese seismic stations (Kik-net and K-net) are compared. FIG. 10 demonstrates that the waveform fit for periods 20-100 sec is good or very good in northern and central parts of the region (Aomori, Iwate and Miyagi prefectures). In the southern part (Fukushima, Ibaraki and Chiba prefectures) the amplitude fit is good, but the delay time of synthetic waveforms is smaller than observed. This model also reproduces qualitatively the multi-seismic wave-front observed from the strong ground motion and GPS data along the Japanese coast; see FIG. 1.

The rupture time is shown in FIG. 9. This sketch reflects the time when the rupture broke the SMGA regions. Additionally we provide the final slip and peak slip rate distributions shown in FIG. 11, and for reference we show final stress drop distribution in FIG. 12, see also TABLE 2. Comparison of the rupture time with the EGF model of Kurahashi and Irikura, 2013[3] for example (see TABLE 3) demonstrates that our improved model reproduces the rupture time of the EGF model.

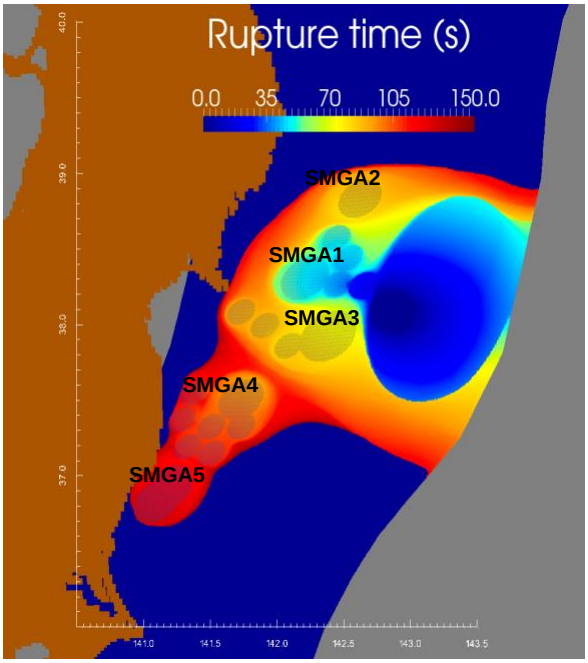

FIG. 9. Dynamic simulation results: Rupture time showing the time when the SMGAs asperities were activated.

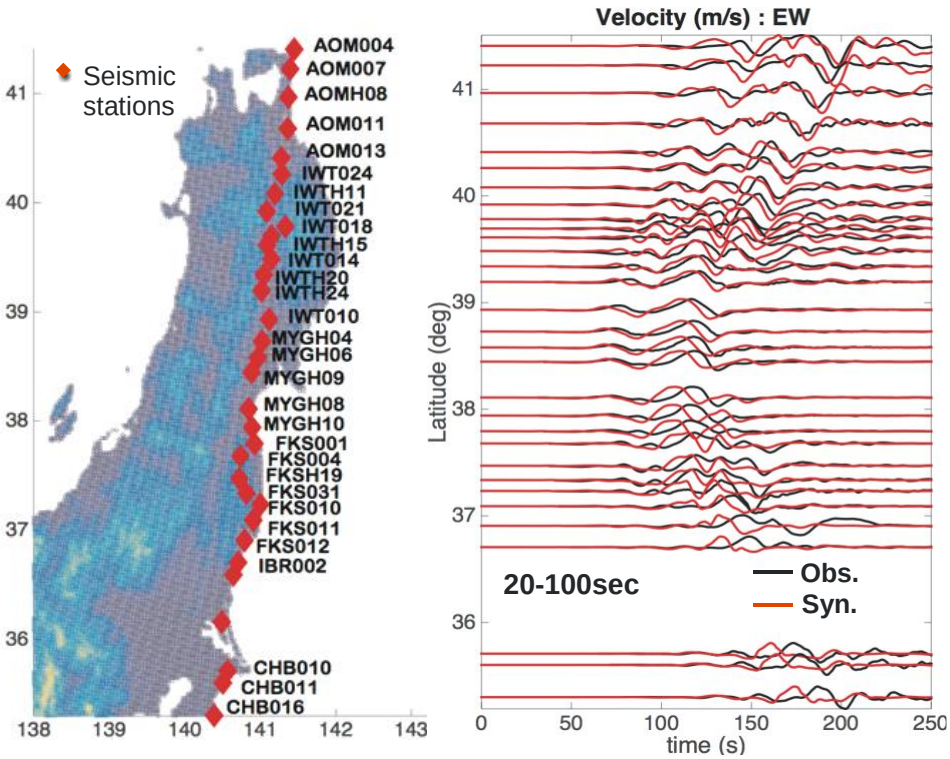

FIG. 10. Comparison of synthetic and recorded seismograms at seismic stations along the Japanese coast shown in FIG. 1. The seismograms are bandpass-filtered from 20 to 100s.

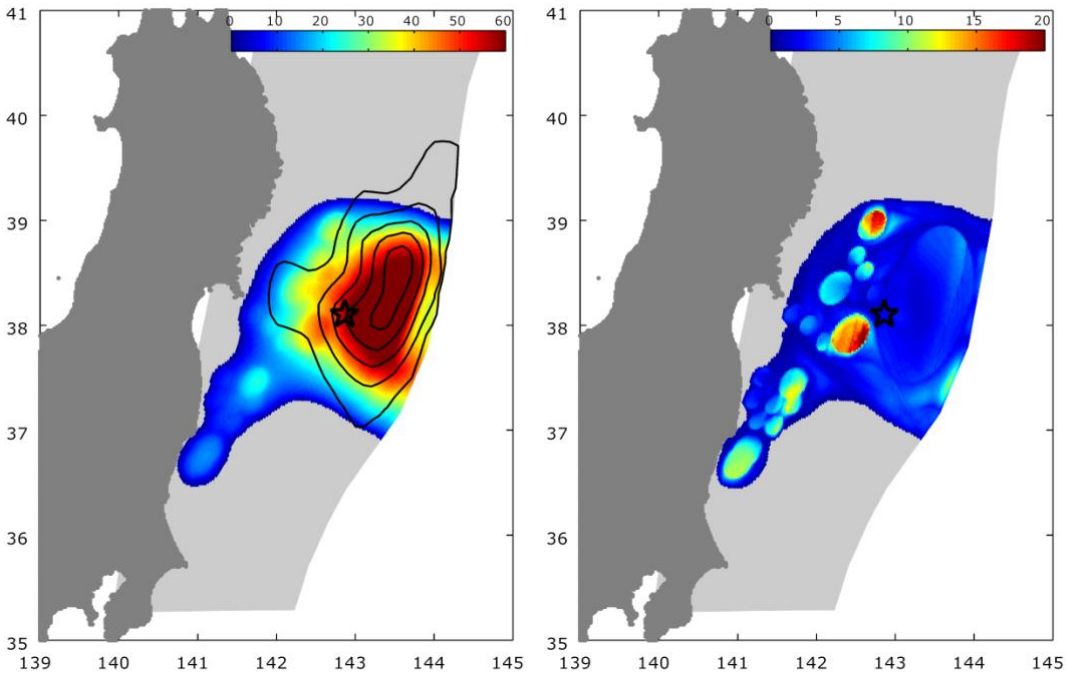

FIG. 11. Dynamic simulation results: (a) final slip (m), and (b) peak slip rate (m/s) distributions. Light gray area is not ruptured.

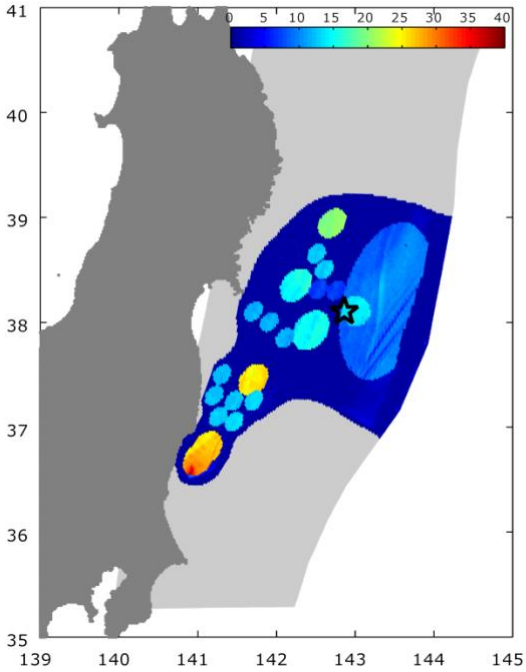

FIG. 12. Dynamic simulation results: final stress drop (MPa) distribution.

TABLE 2**:** STRESS DROP (MPA). DYN : DYNAMIC MODEL (THIS STUDY), K&I : KURAHASHI & IRIKURA, 2013[3].

Model	**SMGA1**	**SMGA2**	**SMGA3**	**SMGA4**	**SMGA5**
Dyn	14.5	20.5	14.7	25	29
K&I	16	20	20	25.2	26

TABLE 3: RUPTURE SEQUENCE (S). DYN : DYNAMIC MODEL, K&I : KURAHASHI & IRIKURA, 2013[3].

Model	**SMGA1**	**SMGA2**	**SMGA3**	**SMGA4**	**SMGA5**
Dyn	38.0	72.0	67.3	106.0	120.0
K&I	24.5	66.5	66.5	117.5	127.5

2.4.3D FDM simulations of short period waves (5~20sec)

The objective of this work is to develop a dynamic model that qualitatively reproduce waveforms in the strong-motion period range. To check if the developed model can reproduce these waveforms, we ran 3D simulations in the 3~20 sec period range using the staggered grid 3D FDM (Graves, 1996; Pitarka, 1999[48, 49]). The 3D velocity structure model is taken from JIVSM which is shown in Figure 10 of Koketsu et al. (2012[50]). FIG. 13 shows a depth cross-section of the JIVSM model through the hypocentral region of Tohoku earthquake. We compare simulation results for envelopes of velocity records, see FIG. 14. Simulated envelopes generally reproduce the observed envelopes, both in amplitude and arrival of the

most intense wave packets WP1, WP2 and WP5. Wave packets WP3 and WP4 are unclear in the 3~20 sec period range. In the southern part of the region, simulated amplitudes are overestimated (FIG. 14).

Overall, we could reproduce the rupture process of the Tohoku earthquake and qualitatively reproduce the recorded multi-seismic wave front detected by the KNET and KiK-net networks, and in this way validate the dynamic rupture model.

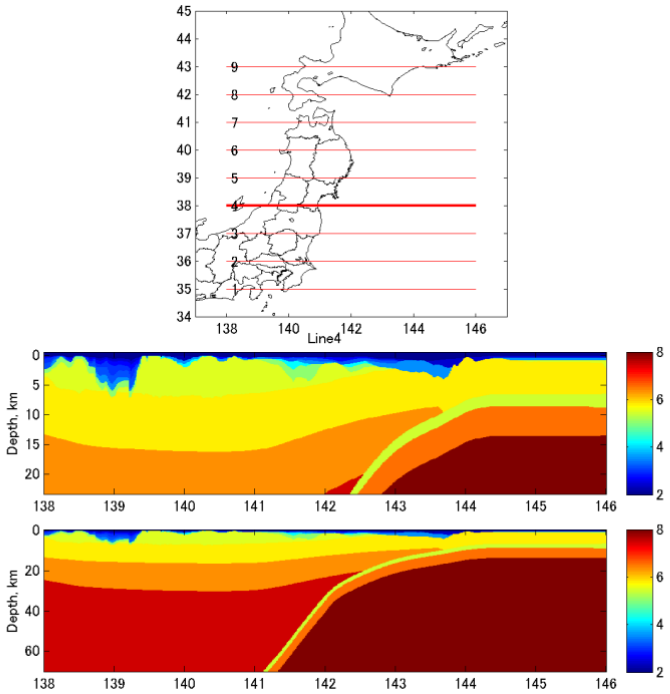

FIG. 13. Cross-section of the 3-D JIVSM velocity structure model in the study region. The location of the cross-section is shown by the red line in the upper panel. Middle and lower panels are P-velocity cross-sections with different depth scales.

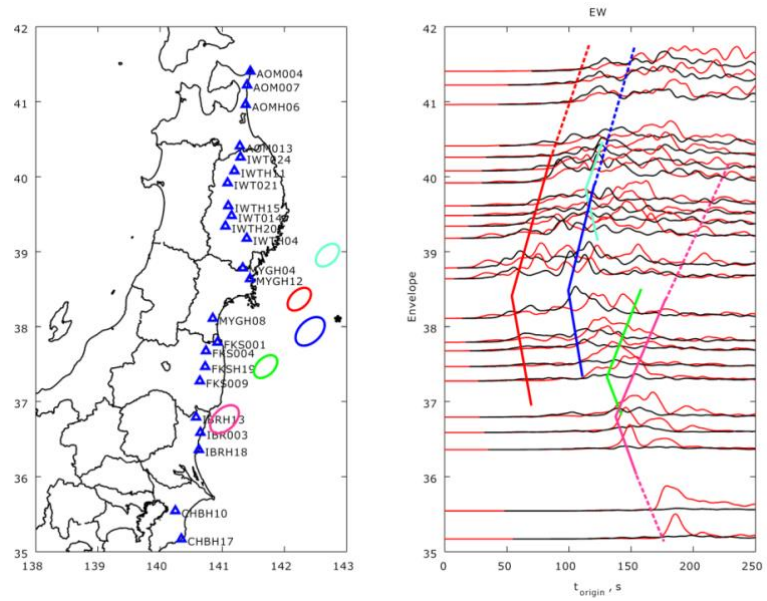

FIG. 14. Comparison of synthetic (red) and recorded (black) short-period envelopes for the line of rock sites along the Japanese coast shown in FIG. 3. Colored lines denotes wave packets WP1-WP5 identified by Kurahashi and Irikura, 2013[3]; dashed segments are our extension. Colored circles correspond to S1-S5 in FIG. 7.

2.5.Discussion

An important contribution of the SMGA's is that they allow the continuous increase in total slip as the rupture keeps growing down-dip. As shown in Figure 13 of Galvez et al. (2016), in the absence of the SMGA asperities, the down-dip rupture arrests once it leaves the shallow slip and ends with lower total slip. Therefore the existence of the SMGA's contributes not only to the ground motions but also to the final earthquake magnitude. In the southern regions, there is an overestimation of peak ground motions due to the values of stress drop prescribed in the SMGA's. Even though the values of stress drop (defined here as: Initial shear stress – normal stress x kinematic friction coefficient) at the SMGA's have been taken from Kurahashi and Irikura, 2013 [3], the dynamic overshoot of slip in dynamic rupture modelling results in larger dynamic stress drop (initial shear stress – final shear stress, computed once the rupture stops). Therefore decreasing the stress drops in the SMGA's will lead to better fitting of ground motions in the southern region.

Among the main targets of dynamic modelling like this one is the "indirect measurement" of parameters that are important for strong ground motion simulation but cannot be estimated or are poorly estimated by direct measurement or kinematic inversion of observational data. One of these is the duration of the source time function (STF): short pulse-like STFs effectively generate short-period strong ground motions, while long smooth STFs only generate long-period ground motions. In previous companion studies (Galvez et al., 2014, 2015[12, 51]), we found that the duration of STFs may correlate well with Dc values. STFs in high Dc asperity A are long and smooth. STFs in low Dc SMGA areas are short and impulsive. Dc is an internal property of the fault and, in contrast to stress distribution for example, it persists through earthquake cycles. This finding (if confirmed) will be invaluable for strong motion predictions (Irikura and Miyake, 2011[52]), because it limits the location of SMGAs of future earthquakes to the location of SMGAs of past earthquakes on the same fault. However, if this is not the case, it may be necessary to vary the location of SMGA's.

Somewhat similar reverse rupture propagation was observed by EGF analysis and ray concentration analysis for the 2007 Niigata-ken Chuetsu-oki earthquake. Kamae and Kawabe, 2008; Petukhin et al., 2009[53, 54], (see also Irikura et al., 2009[55]) found that large ground motions recorded at the Kashiwazaki Kariwa NPP (KKNPP) could be explained better using a source model with 3 asperities and rupture of Asperity 3 toward KKNPP, opposite that of the main rupture. In addition to the 2011 Tohoku earthquake example, the 2007 Chuetsu-oki example shows that reverse rupture propagation may be not rare on heterogeneous faults.

2.6.Conclusions

We performed dynamic rupture simulation of the Tohoku earthquake using spectral element code SPECFEM3D. This tool allows for complex ruptures in subduction zones. Using these capabilities, a down-dip asperities with a bridge by a small high stress drop patches have been introduced to reproduce the observed rupture sequence of SMGAs: Hypocenter-SMGA1-SMGA2&3-SMGA2-SMGA5. The resulting dynamic model successfully reproduced the recorded waveforms in the 20~100 seconds period range. For short period waveform simulation (5~20sec), 3D FDM has been used with a detailed 3D JIVSM velocity model. The peak amplitudes of the simulated short period waveforms generally reproduce the peak amplitudes of the recorded waveforms. However in southern areas they are overestimated due to the larger stress drop in SMGA[3].

Acknowledgement. This study was based on the 2016 research project 'Improvement for uncertainty of strong ground motion prediction' by the Nuclear Regulation Authority (NRA), Japan. The Super Computer Shaheen II at KAUST University has been used to run the models presented in this study. Shaheen II is a Cray XC40 delivering over 7.2 Pflop/s of theoretical peak performance. Overall the system has a total of 197,568 processor cores and 790TB of aggregate memory.

REFERENCES

[1] TAJIMA, F., et al, "A review of the 2011 Tohoku-oki earthquake (Mw 9.0): large-scale rupture across heterogeneous plate coupling", Tectonophysics **586** (2013) 15.

[2] LAY, T., "A review of the rupture characteristics of the 2011 Tohoku-oki Mw 9.1 earthquake", Tectonophysics (2017) http://dx.doi.org/10.1016/j.tecto.2017.09.022.

[3] KURAHASHI, S., IRIKURA, K., "Short Period Source Model of the 2011 Mw 9.0 off the Pacific Coast of Tohoku Earthquake". Bull. Seismol. Soc. Am. **103** (2013) 1373.

[4] KURAHASHI, S., IRIKURA, K., "Source model for generating strong ground motions during the 2011 Off the Pacific Coast of Tohoku earthquake", Earth Planets Space **63** (2011) 571.

[5] KUBO, H., et al., „Period Dependence on Source Process of the 2011 Tohoku Earthquake by Multi Period-band Waveform Inversions", 2013 AGU Fall Meeting, San Francisco (2013) S43A-2469.

[6] YOSHIDA, K., et al., "Source process of the 2011 off the Pacific coast of Tohoku Earthquake inferred from waveform inversion with long-period strong-motion records", Earth Planets Space **63** (2011) 577.

[7] GUSEV, A.A., et al., "Correlation between Local Slip Rate and Local High-frequency Seismic Radiation in an Earthquake Fault", Pure Appl. Geophys. **163** (2006) 1305, DOI 10.1007/s00024-006-0068-4.

[8] SIMONS, M., et al., "The 2011 Magnitude 9.0 Tohoku-Oki Earthquake: Mosaicking the Megathrust from Seconds to Centuries", Science **332** (2011) 1421.

[9] MENG, L., et al., "A window into the complexity of the dynamic rupture of the 2011 Mw 9 Tohoku-Oki earthquake", Geophys. Res. Lett. **38** (2011) L00G07.

[10] HUANG, Y., et al., "Slip-weakening models of the 2011 Tohoku-Oki earthquake and constraints on stress drop and fracture energy", Pure. Appl. Geophys., (2013) 1-14, doi:10.1007/s00024-013-0718-2.

[11] HUANG, Y., et al., "Slip-weakening models of the 2011 Tohoku-oki earthquake and constraints on stress drop and fracture energy", Pure Appl. Geophys. **171** (2014) 2555, http://dx.doi.org/10.1007/s00024-013-0718-2.

[12] GALVEZ, P., et al., "Dynamic earthquake rupture modeled with an unstructured 3D spectral element method applied to the 2011 M9 Tohoku earthquake", Geophys. J. Int. **198** (2014) 1222.

[13] GALVEZ, P., et al., "Rupture Reactivation during the 2011 Mw 9.0 Tohoku Earthquake: Dynamic Rupture and Ground-Motion Simulations", Bull. Seismol. Soc. Am. **106** (2016) 819.

[14] AVOUAC, J.-P., et al., „Lower edge of locked Main Himalayan Thrust unzipped by the 2015 Gorkha earthquake", Nature Geoscience **8** (2015) 708, doi:10.1038/ngeo2518.

[15] SOMERVILLE, P., et al., "Characterizing crustal earthquake slip models for the prediction of strong ground motion", Seism. Res. Lett. **70** (1999) 59.

[16] IRIKURA, K., MIYAKE, H., "Prediction of strong ground motions for scenario earthquakes", Journal of Geography **110** (2001) 849, doi:10.5026/jgeography.110.6_849 (in Japanese with English abstract).

[17] MADARIAGA, R., „Implications of stress-dromp models of earthquakefso for the inversion of stress drop from seismic observations“, Pure Appl. Geophys. **15** (1977) 301.
[18] PULIDO, N., DALGUER, L.-A., “Estimation of the high-frequency radiation of the 2000 Tottori (Japan) earthquake based on the dynamic model of fault rupture: Application to the strong ground motion simulations”, Bull. Seismol. Soc. Am. **99** (2009) 3205, doi : 10.1785/0120080165.
[19] NAKAMURA, H., MIYATAKE, T., “An approximate expression of slip velocity time functions for simulation of near-field strong ground motion”, Zisin **53** (2000) 1 (in Japanese).
[20] HISADA, Y., “A theoretical omega-square model considering the spatial variation on slip and rupture velocity”, Bull. Seism. Soc. Am. **90** (2000) 387.
[21] HISADA, Y., “A theoretical omega-square model considering the spatial variation on slip and rupture velocity. II. Case for a two-dimensional source model”, Bull. Seism. Soc. Am. **91** (2001) 651.
[22] GUATTERI, M., et al., “Strong ground-motion prediction from stochastic?dynamic source models”, Bull. Seism. Soc. Am. **93** (2003) 301.
[23] HEATON, T.H., “Evidence for and implications of self-healing pulses of slip in earthquake rupture”, Phys. Earth Planet. Inter. **64** (1990) 1.
[24] PERRIN, G., et al., “Self-healing slip pulse on a frictional surface”, Journal of the Mechanics and Physics of Solids **43** (1995) 1461.
[25] BEROZA, G.C., MIKUMO, T., “Short slip duration in dynamic rupture in the presence of heterogeneous fault properties”, J. Geophys. Res.: Solid Earth **101** (1996) 22449.
[26] HUANG, Y., AMPUERO, J. P., “Pulse-like ruptures induced by low-velocity fault zones”, J. Geophys. Res. **116** (2011) B12307, doi:10.1029/2011JB008684.
[27] HUANG, Y., et al., “A dynamic model of the frequency-dependent rupture process of the 2011 Tohoku-oki earthquake”, Earth Planets Space **64** (2012) 1061, http://dx.doi.org/10.5047/eps.2012.05.011.
[28] LAY, T., et al., “Depth-varying rupture properties of subduction zone megathrust faults”, J. Geophys. Res. **117** (2012) B04311. http://dx.doi.org/10.1029/2011JB009133.
[29] KANAMORI, H., HEATON, T. “Microscopic and Macroscopic Physics of Earthquakes, Geo-Complexity and the Physics of Earthquakes”, Geophysical Mongraph **120** (2000) 1.
[30] ASANO, K., IWATA, T., “Source model for strong ground motion generation in the frequency range 0.1-10 Hz during the 2011 Tohoku earthquake”, Earth Planets Space **64** (2012) 1111.
[31] SATOH, T., “Source modeling of the 2011 Off the Pacific Coast of Tohoku earthquake using empirical Green’s function method: From the viewpoint of the short-period spectral level of interpolate earthquakes”, J. Struct. Constr. Eng. **675** (2012) 695.
[32] KAWABE, H., KAMAE, K., “Source Modeling of the 2011 Off the Pacific Coast of Tohoku Earthquake”, Journal of Japan Association for Earthquake Engineering **13** (2013) 75 (in Japanese with English abstract).
[33] FUKUYAMA, E., et al., “Automated seismic moment tensor determination by using on-line broadband seismic waveforms”, Zisin **51** (1998) 149 (in Japanese with English abstract).
[34] LEE, S.J., et al., “Evidence of large scale repeating slip during the 2011 Tohoku-Oki earthquake”, Geophys. Res. Lett. **38** (2011) L19306.
[35] YUE, H., LAY, T., “Inversion of high-rate (1-sps) GPS data for rupture process of the 11 March 2011 Tohoku earthquake (Mw 9.1)”, Geophys. Res. Lett. **38** (2011) L00G09, http://dx.doi.org/10.1029/2011GL048700.

[36] SUZUKI, W., et al., “Rupture process of the 2011 Tohoku-Oki mega-thrust earthquake (M9.0) inverted from strong-motion data”, Geophys. Res. Lett. **38** (2011) L00G16.
[37] YAGI, Y., FUKAHATA, Y., “Rupture process of the 2011 Tohoku-oki earthquake and absolute elastic strain release”, Geophys. Res. Lett. **38** (2011) L19307, http://dx.doi.org/10.1029/2011GL048701.
[38] WEI, S., et al., “Sources of the shaking and flooding during the Tohoku-Oki earthquake: A mixture of rupture styles”. Earth. Planet. Sci. Lett. **333-334** (2012) 91.
[39] SATAKE, K., et al., “Time and space distribution of coseismic slip of the 2011 Tohoku earthquake as inferred from tsunami waveform data”, Bull. Seismol. Soc. Am. **103** (2013) 1473, http://dx.doi.org/10.1785/0120120122.
[40] GUSMAN, A.R., et al., “Source model of the great 2011 Tohoku earthquake estimated from tsunami waveforms and crustal deformation data”, Earth Planet. Sci. Lett. **341-344** (2012) 234, http://dx.doi.org/10.1016/j.epsl.2012.06.006.
[41] YAMAZAKI, Y., et al., “Modeling of the 2011 Tohoku near-field tsunami from finite-fault inversion of seismic waves”, Bull. Seismol. Soc. Am. **103** (2013) 1444, http://dx.doi.org/10.1785/0120120103.
[42] PETUKHIN, A., et al., “Tsunami simulation by tuned seismic source inversion for the great 2011 Tohoku earthquake”, Pure Appl. Geophys. **174** (2017) 2891, http://dx.doi.org/10.1007/s00024-017-1611-1.
[43] ISHII, M., “High-frequency rupture properties of the Mw 9.0 Off the Pacific Coast of Tohoku earthquake”, Earth Planets Space **63** (2011) 609.
[44] YAGI, Y., et al., “Smooth and rapid slip near the Japan Trench during the 2011 Tohoku-oki earthquake revealed by a hybrid back-projection method”, Earth Planet. Sci. Lett. **355-356** (2012) 94, http://dx.doi.org/10.1016/j.epsl.2012.08.018.
[45] IDE, S., AOCHI, H., “Historical seismicity and dynamic rupture process of the 2011 Tohoku-Oki earthquake”, Tectonophysics **600** (2013) 1, http://dx.doi.org/10.1016/j.tecto.2012.10.018.
[46] O’HARA, K., et al., “Experimental frictional heating of coal gouge at seismic slip rates: Evidence for devolatilization and thermal pressurization of gouge fluids”, Tectonophysics **424** (2006) 109.
[47] CHEN, X., et al., “Friction Evolution of Granitic Faults: Heating Controlled Transition From Powder Lubrication to Frictional Melt”, J. Geophys. Res. **122** (2017) 9275.
[48] GRAVES, R. W. “Simulating seismic wave propagation in 3D elastic media using staggered-grid finite differences”, Bull. Seismol. Soc. Am. **86** (1996) 1091.
[49] PITARKA, A., “3D finite-difference modeling of seismic motion using staggered grids with nonuniform spacing”, Bull. Seism. Soc. Am. **89** (1999) 54.
[50] KOKETSU, K., et al., “Japan Integrated Velocity Structure Model Version 1”, The 15th World Conference on Earthquake Engineering, (Proc. Conf. Lisbon, 2012), Paper No. 1773.
[51] GALVEZ, P., et al., “Characteristics and waveform simulation for dynamic rupture model of the 2011 Tohoku earthquake with deep SMGAs”, Japan Geoscience Union Meeting 2015, Chiba, Japan (2015) presentation SSS02-10.
[52] IRIKURA, K., MIYAKE, H., „Recipe for predicting strong ground motion from crustal earthquake scenarios“, Pure Appl. Geophys., **168** (2011) 85, doi:10.1007/s00024-010-0150-9.
[53] KAMAE, K., KAWABE, H., Source model and strong motion simulations for the 2007 Niigata-ken Chuetsu earthquake, (in Japanese) (2008) http://www.rri.kyoto-u.ac.jp/jishin/eq/niigata_chuetsuoki_5/chuuetsuoki_20080307.pdf
[54] PETUKHIN, A., et al., “3-D effects of space-time ray concentration on the EGF simulation results: Case of the 2007 Chuetsu-oki earthquake”, Chiba, Japan, (2009)

presentation S152-P003.
[55] IRIKURA, K., et al., “Best-fit source model for simulating strong ground motions from the 2007 Niigata-ken Chuetsu-oki earthquake”, Japan Geoscience Union Meeting 2009, Chiba, Japan, (2009) presentation S152-007.